Progress In Electromagnetics Research B, Vol. 53, 205–221, 2013

LOW MUTUAL COUPLING BETWEEN MIMO ANTENNAS BY USING TWO FOLDED SHORTING STRIPS

Hari S. Singh, Bhaskarareddy Meruva*, Gaurav K. Pandey, Pradutt K. Bharti, and Manoj K. Meshram

Department of Electronics Engineering, IIT (BHU), Varanasi, UP 221005, India

Abstract—This paper presents a compact dual-band multiple input multiple output (MIMO) antenna with low mutual coupling, operating in the 2.4 GHz band (2.4–2.485 GHz) and 5.5 GHz band (5.15–5.85 GHz). The proposed antenna system consists of two antenna elements located at the top two corners of FR4 substrate (PCB). Each element dimension is reduced substantially by employing a folded structure and slots on the top patch plate, so that it takes up a small volume of $12 \times 9 \times 6\,\text{mm}^3$. To enhance port-to-port isolation and efficiency of each antenna, an additional non-radiating folded shorting strip is connected between each antenna element and ground plane of PCB. The measured isolation values are lower than −28 dB over the lower WLAN band (2.4–2.485 GHz) and better than −26 dB (−30 dB in most of the band) across the higher WLAN band (5.15–5.85 GHz). The improvement in antenna's efficiency caused to raise up 1 dB of effective diversity gain of MIMO system. Furthermore, *S*-parameters, radiation patterns and diversity performance characteristics are provided.

1. INTRODUCTION

In today's fast paced world, multiple-input multiple-output (MIMO) technology made a great breakthrough by satisfying the demand of higher quality mobile communication services without using any additional radio resources [1, 2]. The huge potential of MIMO techniques is evidenced by a rapid adoption into the wireless standards, such as WLAN, LTE (Long Term Evolution), and WiMAX. Traditionally, MIMO systems employ multiple antenna elements to send or receive signals. In MIMO systems mutual coupling is a

Received 23 May 2013, Accepted 20 July 2013, Scheduled 29 July 2013

* Corresponding author: Bhaskarareddy Meruva (bhaskarareddy.meruva.ece11@itbhu.ac.in).

well known effect and it becomes more critical when inter-element spacing is very small. This kind of situation can occur in mobile communications, especially in mobile phones, where space limitations become an important variable. In recent years, the interest for multiband multi-antenna systems has been growing for multi standard wireless terminals. In such multiband devices, achieving high isolation between the radiating elements is a challenging task and also it is difficult to control the isolation over the desired bands. So it gives a real challenge to antenna designers to produce an efficient MIMO system.

Some of the solutions have been reported in [3–13] to reduce the mutual coupling between two antenna elements. In [3–7], the mutual coupling was effectively reduced by using defected ground structures (DGS). Antenna array with low mutual coupling, operating at 2.45 GHz is reported in [3], and the improvement of 40 dB isolation is achieved by etching two $\lambda/2$ slots on the ground plane. A combination of rectangular slot ring and inverted T-shaped slot stub has been reported in [4] to reduce the mutual coupling between two quad band antennas. Ground plane with N-section resonator slots [5], protruded T-shaped ground plane [6], and tree-like structure on ground plane [7] were implemented to improve port-to-port isolation. In [8] transmission characteristics of different DGS and their equivalent circuit models were presented. Though DGS provides good isolation characteristic to MIMO antenna systems, it creates difficulties for RF circuits to feed the antenna elements when the solid ground plane is modified or removed.

Electromagnetic band gap (EBG) structures, neutralization techniques, and lumped circuit networks are also attractable solutions to produce high isolation. Some of the EBG structures were reported in [9, 10] to reduce the mutual coupling by suppressing the surface waves. However, EBG structures require an intricate fabrication process and also a large area. Some of the neutralization techniques have been suggested in [11, 12] to improve isolation by utilizing a field cancelling concept. In [11, 12], antennas are designed for the DCS and UMTS bands and studied the mutual coupling between them by considering the feeding strip facing and shorting strip facing cases. They used a single suspended line of different lengths for cancelling the fields and about -20 dB isolation was achieved. The lumped circuit networks presented in [13] are used to provide good isolation of -23 dB between two antenna elements. But the lumped components induce the additional losses, which in turn strongly affect the total antenna efficiencies. So, even if MIMO system exhibits an acceptable isolation among multi-antenna elements, it is necessary to decrease

the antenna's mutual coupling to ensure that less power is lost in the other radiators and, thus, the total efficiencies are maximized. Therefore, here we are proposing a decoupling network which consists of two separate folded shorting strips that effectively maximize the both isolation and the antenna's total efficiency.

In this paper, we present compact dual band PIFA for MIMO applications operating over the IEEE 802.11b/g (2.4–2.48 GHz) and IEEE 802.11a (5.15–5.85 GHz) bands. Initially, the MIMO antenna system consists of two PIFAs, and each one is constructed by E-shaped and folded patch with vertical parasitic strip. This MIMO antenna system is producing acceptable isolation (≤ -15 dB) values by properly placing the antennas on the top corners of the PCB and selecting the positions of the feed points and shorting strips. However, when we place the mobile circuitry like battery, LCD, housing box, camera, sensors, acoustics and other RF circuit elements around the antennas, there may be chance to deteriorate the isolation characteristics. Therefore, here, we proposed a MIMO antenna system with two folded shorting strips of 0.22λ at 2.45 GHz to achieve low mutual coupling to compensate the effect of mobile environment and improve the antenna efficiency which helps to provide the better effective diversity gain. The folded shorting strip is connected between each antenna element (feed strip facing) and PCB ground plane. The idea is to create an additional coupling path such that the ground plane current from port 1 is not entering into port 2 so that a current loop is formed between shorting pin to feed point via folded shorting strip. Thus, the amount of current flowing from port 1 to port 2 is very negligible and it leads to low mutual coupling between two antenna elements. The rest of the paper is structured as follows: Section 2 presents the antenna design and configuration, Section 3 illustrates the parametric study and analyses, the results and discussion in Section 4, and lastly conclusions are drawn in Section 5.

2. ANTENNA DESIGN AND CONFIGURATION

The initial antenna structure shown in Fig. 1(a), consists of two symmetrical back-to-back planar inverted F-antenna (PIFA) elements, which are located on top two corners of the substrate FR4 (PCB of mobile device with $\varepsilon_r = 4.4$ and $\tan\delta = 0.018$). The dimension of substrate is chosen as $100 \times 60 \times 0.8\,\text{mm}^3$ as mobile circuit board. The antenna element is made up of copper sheet with thickness of 0.2 mm. Fig. 1(b) shows the antenna structure with folded shorting strip, which is connected between each antenna element and ground plane. Figs. 2(a)–(c) show the details of single antenna element and its

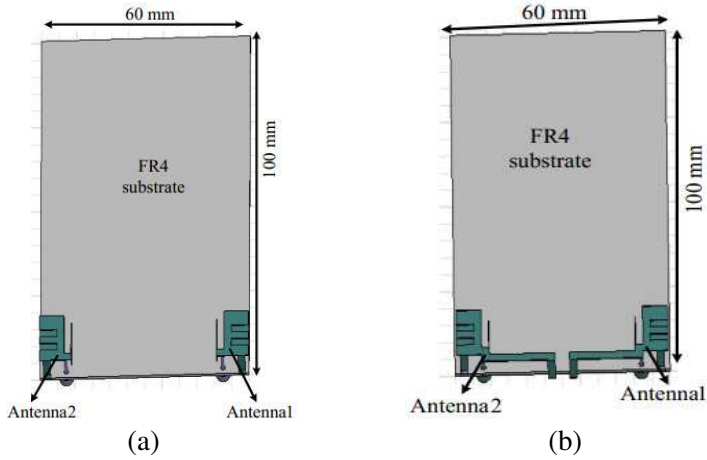

Figure 1. (a) Proposed antenna without folded shorting strip. (b) Proposed structure with folded shorting strip.

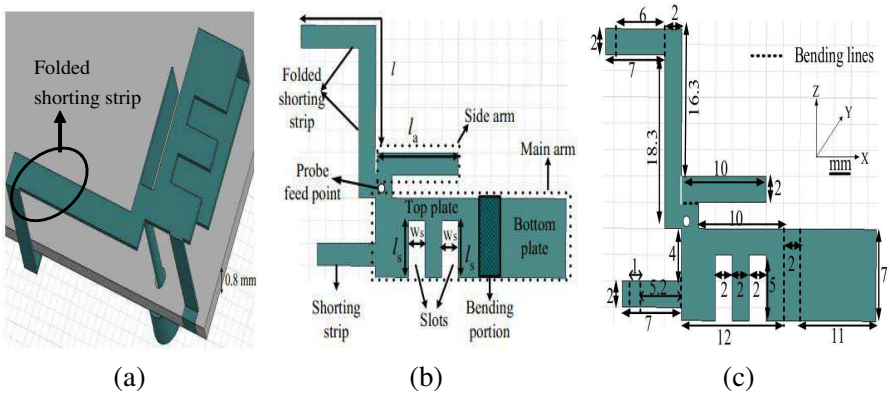

Figure 2. (a) 3-D view of single antenna element. (b) Unfolded planar structure of single antenna element. (c) Optimized dimensions of (b) in mm.

optimized dimension values. Each element comprises of two radiating arms (main arm and side arm) resonating at 2.45 GHz and 5.5 GHz frequencies respectively. By taking into account of mobile space, the main radiating arm is folded and initially it is resonating at 2.75 GHz. In order to resonate at desired frequency (2.45 GHz) two slots are loaded on the top patch plate. These two slots increase the electrical length of radiator and decreases the resonant frequency from 2.75 to 2.45 GHz as shown in Fig. 3(a). The side radiating arm is bent

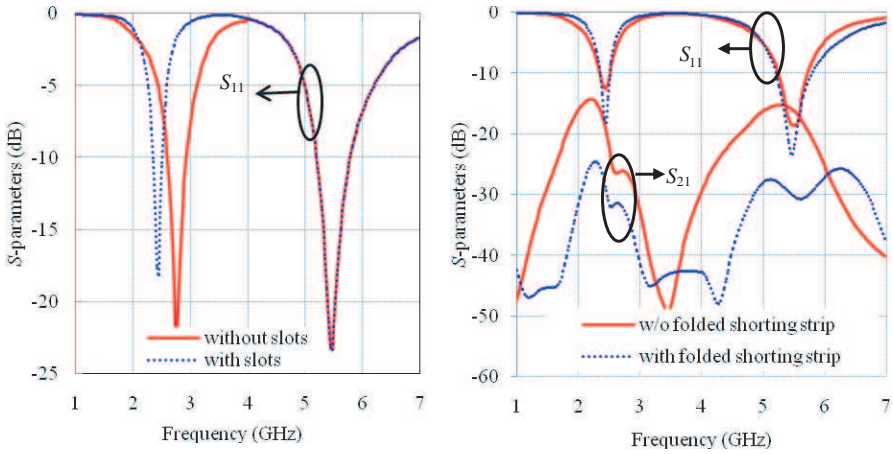

Figure 3. (a) Reflection coefficient versus frequency of Fig. 1(a) without slots on top plate. (b) Comparison of S-parameters of proposed structures without folded shorting strip Fig. 1(a) and with folded shorting strip Fig. 1(b).

vertically along to main arm so as to occupy less space. In such a way we ensured that the compactness of antenna element within $12 \times 9 \times 6\,\text{mm}^3$. The total lengths of the two radiating arms are chosen based on the fundamental PIFA resonant frequency (f_r) equation given as [14].

$$f_r = \frac{c}{4 * (L_1 + L_2)} \tag{1}$$

where, c is velocity of light, L_1 and L_2 are the length and width of the PIFA antenna.

The simulated S-parameters ($|\mathbf{S_{ij}}|$) with and without folded shorting strip are shown in Fig. 3(b). The obtained isolation ($|\mathbf{S_{21}}|$) values are better than $-18\,\text{dB}$ across 2.45 GHz band (2.4–2.485 GHz) and less than $-15\,\text{dB}$ over 5.5 GHz band (5.15–5.85 GHz).

Though these isolation values are acceptable ($\leq -15\,\text{dB}$), when we implement this structure in practical mobile environment (LCD, battery and other RF circuits) there may be a chance to degrade the isolation characteristics and that causes to reduce the antenna total efficiency.

In view of this, we have proposed a subsequent structure shown in Fig. 1(b), which employs a folded shorting strip to reduce the surface current flow between two antenna elements on ground plane. The main role of folded shorting strip is to make a current loop and that avoids

the current flow from port 1 to port 2 so that we can achieve low mutual coupling. The current loop starts from shorting strip and next to ground plane and next to folded shorting strip and towards feed point. The optimized value of the folded shorting strip is 0.22λ at 2.45 GHz. The achieved isolation values with proposed structure are below -28 dB at all operating frequency bands. The enhancement in isolation is 10 dB at 2.45 GHz band and 13 dB at 5.5 GHz band and the improvement in antenna's total efficiency is averagely 10% in both frequency bands. To further investigate the mechanism of the folded shorting strip, the surface current distribution plots and surface current vector plots at different frequency bands are depicted in the upfront section.

3. PARAMETRIC STUDY AND ANALYSES

3.1. Parametric Study of the Proposed Antenna

The simulated results for S-parameters of proposed structure with different slot length (l_s) are shown in Fig. 4(a). It is observed that the lower resonant frequency decreases with increase of slot length l_s. This is due to the fact that the electrical length of main radiating arm increases with l_s. In the upper band the effect of l_s is negligible and the optimized value of l_s is 5 mm. Fig. 4(b) shows the S-parameters for different slot width (w_s) by keeping l_s at 5 mm. The lower band is shifting towards higher frequency while decreasing w_s, and higher band is almost independent of w_s. The reason for frequency shifting is same as l_s. The isolation values remains same for higher band and decreases at lower frequencies. The optimized value for w_s is obtained to be 2 mm. The S-parameters versus frequency for various values of side arm length (l_a) is shown in Fig. 4(c). By fixing the side arm width at 2 mm, the parameter l_a is tuned. It is observed that high resonant frequency decreases with increase of length l_a and there is no significant effect on the isolation. At the lower band the effect of side arm length on reflection and coupling S-parameters is completely insignificant. Fig. 4(d) shows the simulated reflection and coupling S-parameters of proposed structure with folded shorting strip length (l) as a variable. The length of folded shorting strip varies from 0.15λ to 0.24λ, where λ is lower resonating frequency at 2.45 GHz. It is observed that when the length of folded strip is 19 mm (0.15λ) then reflection coefficient becomes distorted at higher frequency due to the resonating behavior of the folded strip whereas, on other values like 0.22λ and 0.24λ, insignificant effect on reflection coefficient whereas the coupling parameter improved almost from -23 dB to -29 dB.

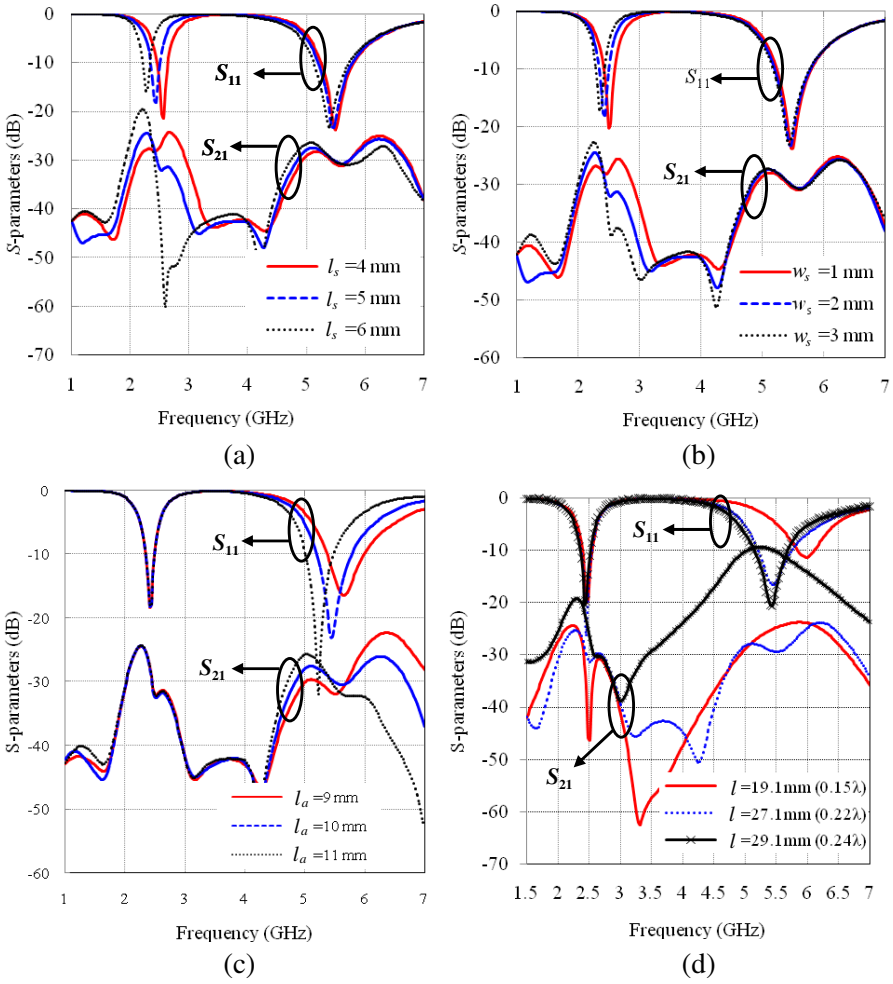

Figure 4. (a) Effect of slot length l_s on S-parameters. (b) Effect of slot width w_s on S-parameters. (c) The S-parameters against side arm length (l_a) variation. (d) The effect of folded shorting strip length (l) on S-parameters.

4. RESULTS AND DISCUSSION

All the simulations have been carried out in Ansoft's HFSS. A prototype of proposed antenna is fabricated and the measurements are done by Agilent Technologies E8364B PNA Network Analyzer. Fig. 5(a) shows the fabricated antenna and size compared with Samsung Galaxy S GT I9000.

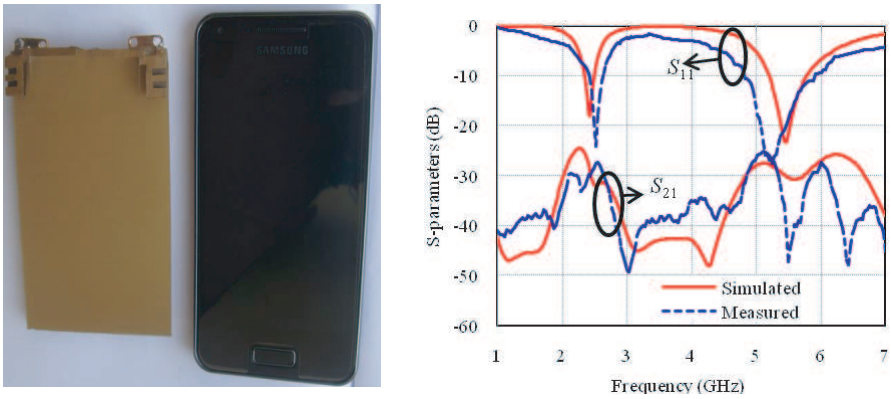

(a) (b)

Figure 5. (a) Prototype of proposed antenna (size compared with Samsung Galaxy S GT I9000). (b) Simulated and measured S-parameters of proposed structure.

4.1. Impedance Performance

Figure 5(b) shows the measured and simulated S-parameters of proposed MIMO antenna. It is observed that the measured results are in good agreement with the simulated results over the lower and higher WLAN bands. The small shift in the resonant frequencies is due to fabrication tolerances.

The measured bandwidth of 290 MHz (2.39–2.68 GHz, 11.4%, VSWR 2.33 : 1) at WLAN (11b/g) band and 1150 MHz (4.85–6 GHz, 21.2%, VSWR 2.33 : 1) at WLAN (11a) band is achieved. The isolation ($|\mathbf{S_{21}}|$) values are down to below -28 dB and -26 dB (-30 dB most of the band) respectively over the aforementioned WLAN bands. This means that the folded shorting strip is providing excellent isolation values by cutting down the surface current flow on ground plane between two antenna elements.

4.2. Surface Current Distribution

The effect of the folded shorting strip is clearly noticed in the surface current distribution plots as shown in Figs. 6(a)–(b). These all plots are taken out when antenna1 is excited and antenna2 is matched terminated. In without folded shorting strip structure a small amount of surface current is coupled from antenna1 to antenna2 through common ground plane. This surface current flow between two ports is reduced to a great extent by the folded shorting strip at all above

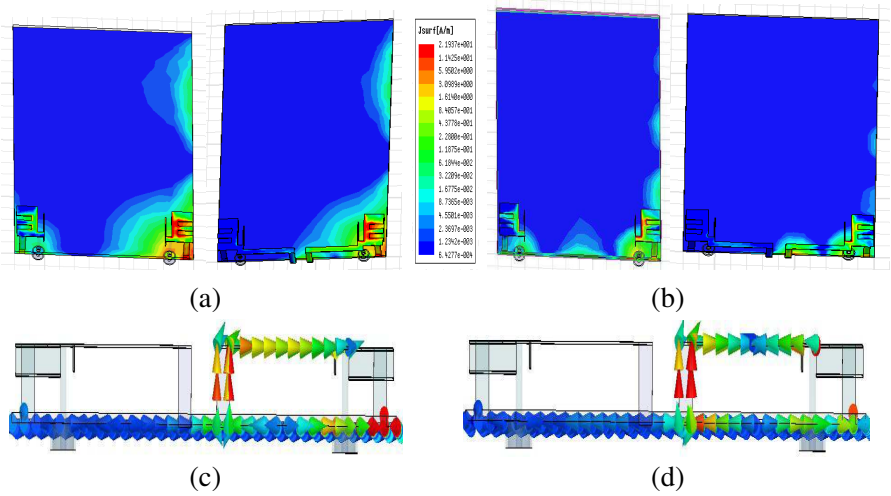

Figure 6. (a) Surface current distribution at 2.45 GHz. (b) Surface current distribution at 5.5 GHz. (c) Surface current flow vector on folded shorting strip at 2.45 GHz. (d) Surface current flow vector on folded shorting strip at 5.5 GHz.

mentioned frequencies and also the effect is same when antenna2 is excited and antenna1 is matched terminated.

From the Figs. 6(c)–(d) it is clearly shown that very less amount of current is flowing towards port 2 and maximum amount of ground current is flowing into folded shorting strip and towards feed point. So the folded shorting strip can significantly increase the isolation of MIMO antenna system.

4.3. Far-field Radiation Pattern

The comparison of simulated and measured radiation patterns of proposed antenna are shown in Figs. 7–8 which represent total field amplitude combining both E_θ and E_ϕ components ($E_{total} = \sqrt{(E_\theta^2 + E_\phi^2)}$). The discrepancy has been observed between simulated and measured results due to the measurement process and limitations of applied numerical techniques in simulation software. During the measurement when antenna1 is excited, antenna2 is matched terminated by 50 Ω load. The radiation patterns in the xz- and yz-plane of antenna1 and antenna2 are the mirror images of each other over the operating frequency bands. That means they are covering the complementary space regions and indicating that the proposed MIMO antenna has good pattern diversity characteristics. In xz-

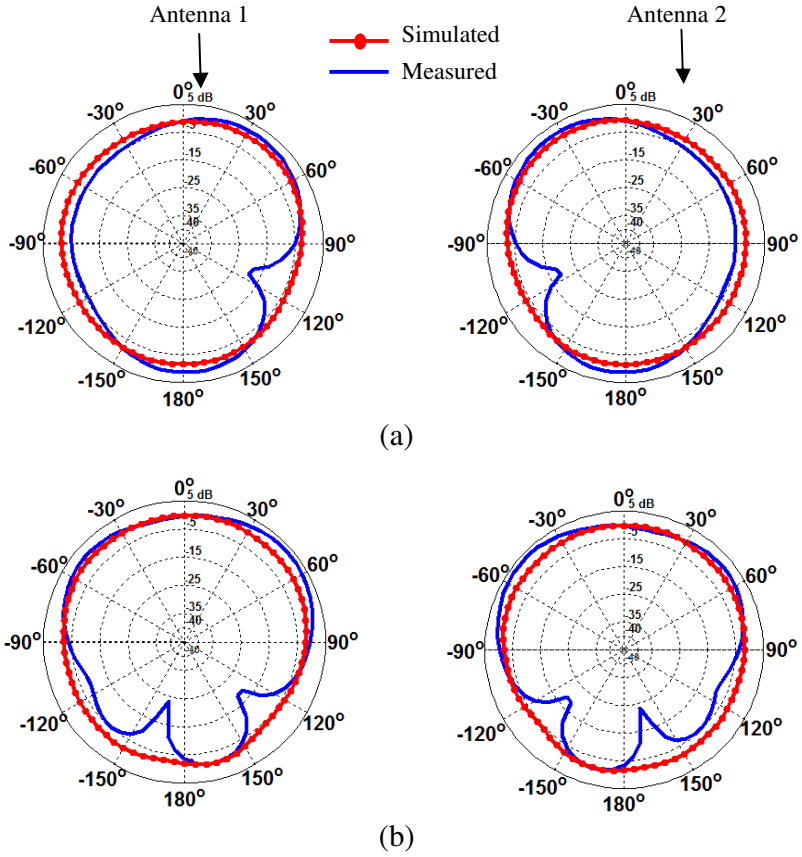

Figure 7. Measured radiation pattern of proposed structure in YZ plane (a) at 2.45 GHz (b) at 5.5 GHz.

and yz-plane the radiation patterns are nearly omni-directional at all interested bands. The antenna peak gains are found to be 4.84 dBi at 2.45 GHz, 5.38 dBi at 5.25 GHz, 5.5 dBi at 5.5 GHz, and 5.4 dBi at 5.8 GHz. The antenna gains are little higher than a regular antenna as a results of ground reflections, low mutual coupling and no surface wave losses. Hence, the MIMO antenna system can probably give high channel capacity.

4.4. Diversity Performance

The mean effective gain (MEG), envelope correlation coefficient (ECC) and diversity gain are the most important parameters for evaluating the MIMO/diversity performances. The diversity parameters have

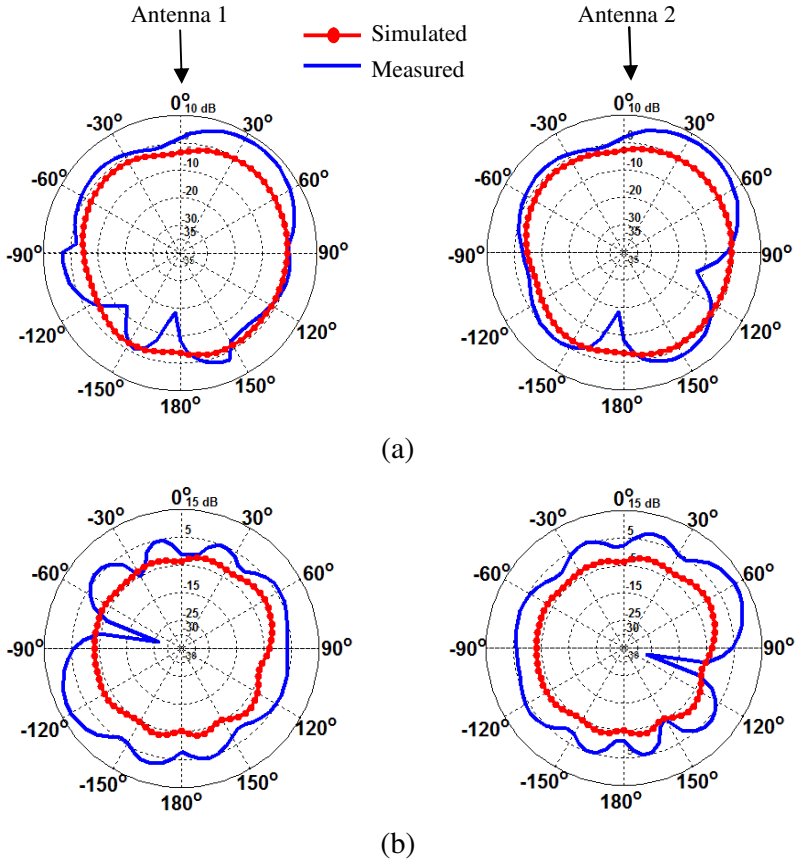

Figure 8. Measured radiation pattern of proposed structure in XZ plane (a) at 2.45 GHz (b) at 5.5 GHz.

been evaluated using CST MWS simulation software [15]. The MEG defined as the ratio between the mean received power of antennas over a random route, and the total mean incident power at the antenna elements. In order to calculate the MEG of a particular antenna element the following expression is used [16].

$$\text{MEG} = \int_0^{2\pi}\int_0^{\pi}\left[\frac{\text{XPR}}{1+\text{XPR}}G_\theta(\theta,\phi)P_\theta(\theta,\phi) + \frac{1}{1+\text{XPR}}G_\phi(\theta,\phi)P_\phi(\theta,\phi)\right]\sin\theta d\theta d\phi \quad (2)$$

where, XPR represents the cross-polarization ratio, G_θ, G_ϕ are the power gain patterns, and P_θ and P_ϕ are the θ- and ϕ-components of angular density functions of the incident power, respectively. It is quite natural to assume that when a mobile user moves randomly in any environment, the incident waves can arise from any azimuth direction with equal probability. However, we can't made such an assumption in elevation direction. A few models have been presented in [17, 18]. The distributions of the angular density functions are depend on the surrounding environment. Some sample statistical models and their typical parameter values for indoor, outdoor, and isotropic environments have been discussed for the angular density functions in [19]. In this paper, P_θ and P_ϕ are assumed to be Gaussian in elevation and uniform in azimuth, and are given by

$$P_\theta(\theta,\phi) = A_\theta \exp\left[\frac{-\left\{\theta-\left(\frac{\pi}{2}-m_v\right)\right\}^2}{2\sigma_v^2}\right], \quad (0\le\theta\le\pi) \tag{3}$$

$$P_\phi(\theta,\phi) = A_\phi \exp\left[\frac{-\left\{\theta-\left(\frac{\pi}{2}-m_H\right)\right\}^2}{2\sigma_H^2}\right], \quad (0\le\theta\le\pi) \tag{4}$$

where, m_v, m_H are, respectively, the mean elevation angles of θ- and ϕ-component wave distribution observed from horizontal direction. σ_v and σ_H are the standard deviations of θ- and ϕ-component wave distributions respectively. A_θ and A_ϕ are constants determined by

$$\int_0^{2\pi}\int_0^{\pi} P_\theta(\theta,\phi)\sin\theta d\theta d\phi = \int_0^{2\pi}\int_0^{\pi} P_\phi(\theta,\phi)\sin\theta d\theta d\phi = 1 \tag{5}$$

Table 1 gives the computed MEG for different XPR at different frequency bands by setting the, $m_v = 10^0$, $m_H = 10^0$, $\sigma_v = 15^0$, and $\sigma_H = 15^0$. By observing the table it is clearly seen that ratio of the MEG1/MEG2 is nearly equal to unity and it indicates that the MIMO system provide the good diversity performance. For calculating ECC we can approach either S-parameters approach or far field pattern data methods. In S-parameters approach the ECC is evaluated using S-parameters of the MIMO system, reported in reference [20] under the following assumptions.

i) the antenna system is a lossless structure, ii) one antenna is excited while the other is terminated with a reference impedance (such as $50\,\Omega$); and iii) the antenna system is in a uniform scattering environment.

$$\rho_e = \frac{\left|S_{11}^* S_{12} + S_{21}^* S_{22}\right|^2}{\left(1-\left(\left|S_{11}^2\right|+\left|S_{21}^2\right|\right)\right)\left(1-\left(\left|S_{22}^2\right|+\left|S_{12}^2\right|\right)\right)} \tag{6}$$

Table 1. Computed MEGs at different frequency bands for different XPRs.

Frequency (GHz)	Indoor (XPR = 5 dB)		Outdoor (XPR = 1 dB)		Isotropic (XPR = 0 dB)	
	MEG1	MEG2	MEG1	MEG2	MEG1	MEG2
2.45	−6.015	−6.150	−5.367	−5.412	−5.2	−5.2
5.25	−3.189	−3.190	−3.796	−3.896	−3.985	−3.85
5.5	−3.184	−3.185	−3.805	−3.812	−3.996	−3.981
5.8	−3.048	−3.150	−3.706	−3.720	−3.911	−3.950

The above equation is valid for ideal antenna cases but practically the mobile terminal antenna's efficiency is not ideal in multipath propagation environment. Therefore, it is not possible to satisfy the i) and iii) assumptions. So here we are going with far field pattern approach [16], in which the envelope correlation coefficient (ρ_e) given in terms of complex cross correlation (ρ_c)

$$\rho_e \approx |\rho_c|^2 \tag{7}$$

under the assumption that the received signals have a Rayleigh distributed envelope and randomly distributed phase. The complex cross correlation ρ_c is evaluated using radiation pattern given in [1]

$$\rho_c = \frac{\int\limits_0^{2\pi} A_{12}(\phi)\, d\phi}{\left[\int\limits_0^{2\pi} A_{11}(\phi)\, d\phi \int\limits_0^{2\pi} A_{22}(\phi)\, d\phi\right]^{1/2}} \tag{8}$$

where, $A_{pq}(\phi) = \text{XPR} * E_{\theta p}(\frac{\pi}{2}, \phi) E^*_{\theta q}(\frac{\pi}{2}, \phi) + E_{\phi p}(\frac{\pi}{2}, \phi) E^*_{\phi q}(\frac{\pi}{2}, \phi)$ and $\overrightarrow{E_p}(\theta, \phi) = E_{\theta p}(\theta, \phi)\hat{\theta} + E_{\phi p}(\theta, \phi)\hat{\phi}$ and is the vector radiation pattern of antenna $p = 1, 2$.

The frequency versus ECC is shown in Fig. 9. The envelope correlation coefficient values are lower than 0.01 over all above mentioned frequency bands and it gives the good diversity gain of MIMO system.

The next important diversity parameter is apparent diversity gain (G_{app}) and is given in terms of correlation coefficient [21]

$$G_{app} = 10 * e_\rho \tag{9}$$

where 10 is the maximum apparent diversity gain at the 1% probability level with selection combining and e_ρ the diversity gain reduction factor

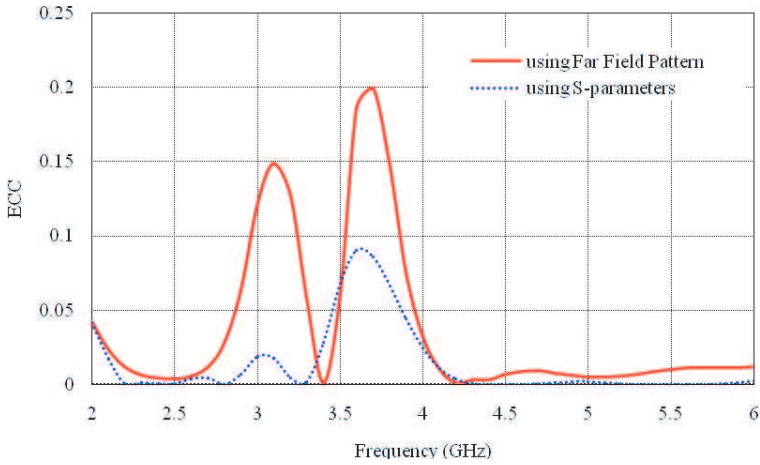

Figure 9. Variation of ECC with frequency.

due to correlation between the signals on the two antennas. e_ρ is given by [22]

$$e_\rho = \sqrt{1 - |\rho_e|^2} \tag{10}$$

The apparent diversity gain does not include the antenna radiation efficiency. The total efficiency of an antenna is given as the total radiated power divided by the incident power at the feed. It includes reflection losses due to the mismatch between the cable and the antenna, as well as dielectric and conduction losses. In MIMO antenna systems, isolation is an additional factor to consider, because the energy of one antenna can couple to another antenna. So that the total efficiency of antenna (η_{total}) is given by [23]

$$\eta_{total} = \eta \left(1 - |S_{11}|^2 - |S_{21}|^2\right) \tag{11}$$

where, η is radiation efficiency of antenna. The impact of folded shorting strip on total efficiency is clearly noticeable from Table 2. The improvement of 10% averagely in total efficiency over the desired bands is due to the fact that the folded shorting strip structure providing good matching conditions to PIFA and also producing the good return loss and isolation characteristics compared to without folded shorting strip structure. The effective diversity gain (EDG) of antenna system is determined by multiplying the diversity gain with total antenna efficiency. From the Table 2, it is clearly observed that the folded shorting strip structure brings the improvement of 1 dB in EDG.

Table 2. The effect of folded shorting strip on diversity gain, and effective diversity gain.

Frequency (GHz)	Without folded shorting strip			With folded shorting strip		
	DG (dB)	η_{total} (%)	EDG (dB)	DG (dB)	η_{total} (%)	EDG (dB)
2.45	9.997	78.0	7.79	9.999	86.0	8.60
5.25	9.996	79.0	7.89	9.999	90.4	9.04
5.5	9.999	90.0	8.99	9.999	99.0	9.89
5.8	9.999	81.6	8.15	9.999	91.0	9.09

5. CONCLUSION

In this paper, a compact dual band MIMO antenna with low mutual coupling operating over WLAN bands (2.4–2.485 GHz and 5.15–5.85 GHz) is proposed. The measured 6-dB return loss bandwidths are 510 MHz and 1700 MHz over lower and higher resonating frequencies respectively. Excellent isolation is achieved between two antenna elements by folded shorting strip. The antenna total efficiencies are improved 10% averagely over the operating frequency bands, and also the improved isolation values are less than −28 dB at WLAN 11.b/g band and better than −26 dB (−30 dB in most of the band) across WLAN 11.a band. The radiation patterns of two antennas are providing good pattern diversity characteristics and also we obtained excellent ECC (lower than 0.01), well diversity gains and the satisfactory MEG ratios over the frequency of interested bands. These indicate that our proposed antenna has a good MIMO/diversity performance and suitable for mobile handset applications.

ACKNOWLEDGMENT

Authors are thankful to Dr. Babau R. Vishvakarma, Emeritus Professor, Indian Institute of Technology (Banaras Hindu University), Varanasi, India for fruitful discussions and suggestions.

REFERENCES

1. Vaughan, R. G. and J. B. Anderson, "Antenna diversity in mobile communications," *IEEE Trans. Veh. Tech.*, Vol. 36, No. 4, 149–172, Nov. 1987.
2. Foschini, G. J. and M. J. Gans, "On limits of wireless communication in a fading environment when using multiple antennas," *Wireless Pers. Commun.*, Vol. 6, No. 3, 311–335, 1998.
3. Sonkki, M. and E. Salonen, "Low mutual coupling between monopole antennas by using two slots," *IEEE Antennas Wireless Propag. Lett.*, Vol. 9, 138–141, 2010.
4. Meshram, M. K., R. K. Animeh, A. T. Pimpale, and N. K. Nikolova, "A novel quad-band diversity antenna for LTE and Wi-Fi applications with high isolation," *IEEE Trans. Antennas Propag.*, Vol. 60, No. 9, 4360–4371, Sep. 2012.
5. Chiu, C.-Y., C.-H. Cheng, R. D. Murch, and C. R. Rowell, "Reduction of mutual coupling between closely-packed antenna elements," *IEEE Trans. Antennas Propag.*, Vol. 55, No. 6, 1732–1738, Jun. 2007.
6. Wu, T.-Y., S.-T. Fang, and K.-L. Wong, "A printed diversity dual band monopole antenna for WLAN operation in the 2.4 and 5.2 GHz bands," *Microwave Opt. Technol. Lett.*, Vol. 36, No. 6, 436–439, Mar. 2003.
7. Zhang, S., Z. Ying, J. Xiong, and S. He, "Ultra-wide band MIMO/diversity antennas with a tree-like structure to enhance wideband isolation," *IEEE Antennas Wireless Propag. Lett.*, Vol. 8, 1279–1283, 2009.
8. Weng, L. H., Y. C. Guo, X. W. Shi, and X. Q. Chen, "An overview on defected ground structure," *Progress In Electromagnetics Research B*, Vol. 7, 173–189, 2008.
9. Makinen, R., V. Pynttari, J. Heikkinen, and M. Kivikoski, "Improvement of antenna isolation in hand-held devices using miniaturized electromagnetic band-gap structures," *Microw. Opt. Technol. Lett.*, Vol. 49, No. 10, 2508–2513, Oct. 2007.
10. Hsu, C.-C., K.-H. Lin, H.-L. Su, H.-H. Lin, and C.-Y. Wu, "Design of MIMO antennas with strong isolation for portable applications," *Proc. IEEE AP-S*, 1–4, Charleston, SC, Jun. 2009.
11. Diallo, A., C. Luxey, P. Le Thuc, R. Staraj, and G. Kossiavas, "Study and reduction of the mutual coupling between two mobile phone PIFAs operating in the DCS1800 and UMTS bands," *IEEE Trans. Antennas Propag.*, Vol. 54, No. 11, 3063–3074, Nov. 2006.

12. Luxey, C. and D. Manteuffel, "Highly efficient multiple antennas for MIMO-systems," *Proc. IEEE iWAT*, 1–3, Lisbon, Portugal, Mar. 2010.
13. Chen, S.-C., Y.-S. Wang, and S.-J. Chung, "A decoupling technique for increasing the port isolation between two strongly coupled antennas," *IEEE Trans. Antennas Propag.*, Vol. 56, No. 12, 3650–3658, Dec. 2008.
14. Saidatul, N. A., A. A. H. Azremi, R. B. Ahmad, P. J. Sohand, and F. Malek, "Multiband fractal planar inverted F antenna (F-PIFA) for mobile phone application," *Progress In Electromagnetics Research B*, Vol. 14, 127–148, 2009.
15. CST Microwave Studio, [online], available: http://www.cst.com.
16. Taga, T., "Analysis for mean effective gain of mobile antennas in land mobile radio environments," *IEEE Trans. Veh. Tech.*, Vol. 39, No. 2, 117–131, May 1990.
17. Dong, L., H. Ling, and R. W. Heath, "Multiple-input multiple-output wireless communication systems using antenna pattern diversity," *Proc. IEEE Global Telecommun. Conf.*, Vol. 1, 997–1001, Taipei, Taiwan, Nov. 2002.
18. Pedersen, K., P. Mogensen, and B. Fleury, "Power azimuth spectrum in outdoor environments," *Electron. Lett.*, Vol. 33, No. 18, 1583–1584, Aug. 1997.
19. Karaboikis, M. P., V. C. Papamichael, G. F. Tsachtsiris, C. F. Soras, and V. T. Makios, "Integrating compact printed antennas onto small diversity/MIMO terminals," *IEEE Trans. Antennas Propag.*, Vol. 56, No. 7, 2067–2078, Jul. 2008.
20. Jusoh, M., M. F. Jamlos, M. R. Kamarudin, and F. Malek, "A MIMO antenna design challenges for UWB applications," *Progress In Electromagnetics Research B*, Vol. 36, 357–371, 2012.
21. Schwartz, M., W. R. Bennett, and S. Stein, *Communication System and Techniques*, 470–474, McGraw-Hill, New York, 1965.
22. Pierce, J. N. and S. Stein, "Multiple diversity with non independent fading," *IRE Proc.*, Vol. 48, 89–104, Jan. 1960.
23. Rao, Q. and K. Wilson, "Design, modeling, and evaluation of a multiband MIMO/diversity antenna system for small wireless mobile terminals," *IEEE Trans. on Components, Packaging and Manufacturing Tech.*, Vol. 1, No. 3, Mar. 2011.